HHS Public Access

Author manuscript

Dev Biol. Author manuscript; available in PMC 2016 December 15.

Published in final edited form as:

Dev Biol. 2015 December 15; 408(2): 292–304. doi:10.1016/j.ydbio.2015.03.013.

ATP4a is required for development and function of the Xenopus mucociliary epidermis - a potential model to study proton pump inhibitor-associated pneumonia

Peter Walentek[1,2,*], **Tina Beyer**[1,3], **Cathrin Hagenlocher**[1], **Christina Müller**[1], **Kerstin Feistel**[1], **Axel Schweickert**[1], **Richard M. Harland**[2], and **Martin Blum**[1]

[1]Institute of Zoology, University of Hohenheim, Garbenstrasse 30, 70593 Stuttgart, Germany

[2]Department of Molecular and Cell Biology, Center for Integrative Genomics, University of California at Berkeley, Berkeley, California 94720, USA

Abstract

Proton pump inhibitors (PPIs), which target gastric H^+/K^+ATPase (ATP4), are among the most commonly prescribed drugs. PPIs are used to treat ulcers and as a preventative measure against gastroesophageal reflux disease in hospitalized patients. PPI treatment correlates with an increased risk for airway infections, i.e. community- and hospital-acquired pneumonia. The cause for this correlation, however, remains elusive. The Xenopus embryonic epidermis is increasingly being used as a model to study airway-like mucociliary epithelia. Here we use this model to address how ATP4 inhibition may affect epithelial function in human airways. We demonstrate that atp4a knockdown interfered with the generation of cilia-driven extracellular fluid flow. ATP4a and canonical Wnt signaling were required in the epidermis for expression of foxj1, a transcriptional regulator of motile ciliogenesis. The ATP4/Wnt module activated foxj1 downstream of ciliated cell fate specification. In multiciliated cells (MCCs) of the epidermis, ATP4a was also necessary for normal myb expression, apical actin formation, basal body docking and alignment of basal bodies. Furthermore, ATP4-dependent Wnt/β-catenin signaling in the epidermis was a prerequisite for foxa1-mediated specification of small secretory cells (SSCs). SSCs release serotonin and other substances into the medium, and thereby regulate ciliary beating in MCCs and protect the epithelium against infection. Pharmacological inhibition of ATP4 in the mature mucociliary epithelium also caused a loss of MCCs and led to impaired mucociliary clearance. These data strongly suggest that PPI-associated pneumonia in human patients might, at least in part, be linked to dysfunction of mucociliary epithelia of the airways.

[*]To whom correspondence should be addressed: walentek@berkeley.edu.

[3]Current address: Medical Proteome Center, Institute for Ophthalmic Research, University of Tübingen, Nägelestrasse 5, 72074 Tübingen, Germany.

Authors contribution

PW initiated, conducted and analyzed experiments. TB performed electron microscopy. CH and KF helped significantly with ependymal flow analysis. CM contributed to ATP4 inhibitor experiments. PW, AS and MB planned experiments and interpreted the results. RMH helped with interpretation of data and writing of the manuscript. PW and MB wrote the manuscript with input from all authors.

Keywords

ATP4; proton pump inhibitor; cilia; small secretory cells; Wnt; Xenopus laevis

Introduction

Proton pump inhibitors (PPIs) are a class of therapeutic drugs used during treatment of gastric and peptic ulcers (Shin and Sachs, 2006). In addition, PPIs are prescribed to hospitalized patients to prevent gastroesophageal reflux disease (GERD) (Fohl and Regal, 2011). PPIs, e.g. Omeprazole, belong to the most widely prescribed drugs, with a worldwide volume of >26 billion US $ and >53 million annual prescriptions in the United States alone (IMS Institute for healthcare informatics, 2011; Reimer, 2013). PPIs inhibit gastric H+/K+ATPase (ATP4) function (Shin et al., 2009). ATP4 is a transmembrane proton pump composed of two catalytic α (ATP4a) and two accessory β (ATP4b) subunits (Shin and Sachs, 1996). ATP4 is highly expressed in the vertebrate stomach and required for acidification of the gastric lumen (Sawaguchi et al., 2004; Shin et al., 2009). In addition to gastric expression of ATP4, it is proposed that ATP4 is expressed in the airways, though these findings are still under debate (Altman et al., 2007; Fischer and Widdicombe, 2006; Herrmann et al., 2007). PPI administration correlates with an increased risk for hospital- and community-acquired pneumonia (Fohl and Regal, 2011). Depending on study design, daily dose, and duration of PPI treatment, the increased risk of developing pneumonia is substantial, but is highly variable (0.91–6.53 fold; confidence interval 95%; de Jager et al., 2012; Fohl and Regal, 2011; Herzig et al., 2014; Jena et al., 2013; Ramsay et al., 2013; Sheen and Triadafilopoulos, 2011). Proposed molecular mechanisms include effects on the immune system or bacterial overgrowth in the stomach, due to increase in gastric pH, enrichment of potential pathogenic microorganisms, and subsequent microaspiration causing airway infections (Fohl and Regal, 2011; Herzig et al., 2014; Reimer, 2013).

The mammalian epithelial lining of the upper respiratory tract constitutes a mucociliary epithelium, which functions as a first line defense against pathogens (Crystal et al., 2008; Mall, 2008; Proud and Leigh, 2011). Dysfunction of the airway mucociliary epithelium causes an increased susceptibility to pulmonary infections (Fliegauf et al., 2007). The Xenopus embryonic epidermis resembles mammalian airway epithelia in many ways, and over the past years it has emerged as an important model for the study of development and function of vertebrate mucociliary epithelia (Hayes et al., 2007; Werner and Mitchell, 2012). It is composed of four cell types: multiciliated cells (MCCs), small secretory cells (SSCs), ion secreting cells (ISCs), and outer/goblet cells (Dubaissi and Papalopulu, 2011; Dubaissi et al., 2014; Quigley et al., 2011; Stubbs et al., 2006; Walentek et al., 2014). The apical surface of MCCs is typically decorated with hundreds of motile cilia, whose coordinated beating causes extracellular fluid flow (Mall, 2008; Marshall and Kintner, 2008); the other cell types of mucociliary epithelia secrete substances like mucus and contribute to the airway surface liquid, thereby protecting the epithelium from inhaled particles and pathogens (Crystal et al., 2008; Jeffery and Li, 1997).

Our previous work has revealed that ATP4 is required for cilia-dependent development of the left-right (LR) body asymmetry in Xenopus: During gastrulation, ATP4-function is a prerequisite for activation of canonical Wnt/β-catenin signaling and expression of foxj1 (Walentek et al., 2012), a master transcription factor for motile ciliogenesis (Stubbs et al., 2008; Yu et al., 2008). LRP6 also cooperates in specification of MCCs in the neurula epidermis (Huang and Niehrs, 2014). Polarization of cilia at the gastrocoel roof plate is mediated by non-canonical Wnt/planar cell polarity (PCP), and this requires ATP4a function as well (Walentek et al., 2012).

Based on the role of ATP4 in motile ciliogenesis and the rationale that the Xenopus epidermis might provide insights into the underlying mechanisms of PPI-associated pneumonia, we tested the role of ATP4 and Wnt signaling in development and function of the mucociliary epithelium. Our results argue for a general role of ATP4 and Wnt signaling in motile ciliogenesis during Xenopus development and in the specification of epidermal SSCs. Pharmacological inhibition of ATP4 after development of the mucociliary epidermis also affected extracellular fluid flow. Therefore, we hypothesize that PPI-associated pneumonia might be in part caused by dysfunction of the mucociliary airway epithelium.

Results

ATP4 is required for normal development of the Xenopus embryonic epidermis

To investigate the potential function of ATP4 in formation of the ciliated Xenopus embryonic epidermis, we analyzed the expression of ATP4a protein in the epidermal ectoderm (Fig. S1). ATP4a was found throughout the animal hemisphere during gastrulation (Fig. S1A, A′) and neurulation (Fig. S1B, C), within the outer and deep layer of the skin ectoderm (Fig. S1B). The deep layer forms multiciliated cells (MCCs), ion secreting cells (ISCs) and small secretory cells (SSCs) which later intercalate into the outer epithelium (Deblandre et al., 1999; Dubaissi et al., 2014, Stubbs et al., 2006). Furthermore, ATP4a protein was enriched in the epidermal ectoderm during neurulation (Fig. S1C), and continued expression in the epidermis throughout tailbud (Fig. S1D) and early tadpole stages (Fig. S1F, G).

The functional relevance of ATP4 for epidermal development and ciliation was tested by morpholino oligonucleotide (MO) mediated knockdown of atp4a (Walentek et al., 2012). Unilateral injections of atp4aMO were targeted to the skin ectoderm (confirmed in all experiments by analysis of co-injected lineage tracer). Morphological analysis by scanning electron microscopy revealed fewer and shorter cilia projecting from the apical surface of individual MCCs and reduced numbers of SSCs (Fig. 1A, B). Ciliation defects in atp4a morphants, together with our previous finding of ATP4a-dependent foxj1 expression during gastrulation (Walentek et al., 2012), suggested that foxj1 expression might also be affected in ATP4a-deficient MCCs; indeed in situ hybridization showed that knockdown of atp4a on the injected side resulted in a downregulation of foxj1 expression, as compared to the contralateral uninjected side (Fig. 1C) or to control morpholino (CoMO) injected specimens ($p<0.001$; Fig. S2A). Reduced numbers of SSCs in the epidermis further indicated possible defects in SSC specification. Expression of foxa1 determines SSC specification (Dubaissi et al., 2014), and in agreement with the morphological data, on average only 50% of foxa1

expressing cells were detected on the atp4aMO injected side as compared to the control side (Fig. 1C; Fig. S2B). In contrast to MCCs and SSCs, ion secreting cells (ISCs) did not show obvious defects, as judged by morphology (Fig. 1A, B) and expression of both the ISC regulator foxi1 (Fig. 1C; Fig. S2C; Quigley et al., 2011) and the ISC marker vH^+ATPase (atp6 subunit expression, Quigley et al., 2011) (Fig. S2D).

These findings were validated by quantitative reverse-transcription PCR (qRT-PCR) (Fig. S3). We used control and injected animal cap explants, which develop into mucociliary epithelium in culture (Sive et al., 2000; Werner and Mitchell, 2013). Four time points were chosen for the analysis: stage 10 (early cell type specification), stage 19 (late specification/ early intercalation), stage 25 (late intercalation, when basal bodies are docked to the apical membrane and ciliogenesis starts), and stage 32 (fully ciliated and functional mucociliary epithelium) (Avasthi and Marshall, 2012; Song et al., 2014; Stubbs et al., 2006). Expression levels were calculated relative to stage 10 uninjected control samples in order to reflect the expression dynamics.

Expression of three major transcriptional regulators in MCCs was analyzed: multicilin (mci; (Stubbs et al., 2012), myb (Tan et al., 2013) and foxj1 (Fig. S2C). mci was only weakly expressed at stage 10, peaked at stage 19 and was barely detectable at later stages (25 and 32) of mucociliary development. The atp4a morphant explants did not display significant changes in mci expression at stages 10 and 19, but there was a slight increase at stages 25 and 32 relative to controls (Fig. S3A). Morphant explants strongly downregulated myb and foxj1 during cell type specification and intercalation stages, but these recovered to normal or above-normal levels by stage 32 (Fig. S3A). These results indicated that not Mci-dependent MCC specification was affected in atp4a morphants, but downstream gene expression of foxj1 and myb, which are required for MCC ciliation. SSCs are induced later during development, compared to MCCs or ISCs (Dubaissi et al., 2014; Walentek et al., 2014). Accordingly, foxa1 expression was highest at stage 25 (Fig. S3B). foxa1 expression was markedly reduced by atp4aMO injections at stages 19 and 25. Furthermore, expression of tph1 (Tryptophan hydroxylase 1; a rate-limiting enzyme for serotonin synthesis and SSC marker; Walentek et al., 2014) was strongly reduced in explants derived from atp4a morphants. In contrast, atp4a knockdown did not negatively affect foxi1 expression (Fig. S3C).

We therefore conclude that although ATP4a is not required for mci expression, it is required for MCC ciliation and SSC specification. In contrast it is not needed for specification of ISCs and ISC-specific gene expression.

ATP4-dependent Wnt/β-catenin signaling regulates foxj1 expression in epidermal MCCs

Confocal imaging of immunostained control and atp4a morphant specimens confirmed a defect in ciliation following atp4a knockdown (Fig. 2A, B), rather than defective specification or intercalation of these cells. In contrast to MCCs of control specimens, which show the characteristic ciliary tuft projecting from the apical membrane of the cell, immunostaining for acetylated-α–tubulin (tubulin) in atp4a morphant MCCs revealed intracellular accumulation of tubulin, but few or no cilia projecting from the apical surface (Fig. 2A). ATP4a-deficient MCCs also showed impaired formation of the apical actin

meshwork (Fig. 2A). This phenotype was reminiscent of the airway MCC phenotype in foxj1 knock-out mice (Gomperts et al., 2004). Loss of foxj1 in mouse airway MCCs causes ciliation defects due to impaired basal body docking to the apical membrane, a prerequisite for motile cilia formation (Gomperts et al., 2004; Marshall, 2008). We therefore investigated whether ciliation defects correlated with defects in basal body localization in atp4a morphants. Embryos were co-injected with a sas6-gfp construct in order to label basal bodies (Klos Dehring et al., 2013), and ciliation was analyzed in parallel by tubulin staining (Fig. 2B). Sas6-GFP positive basal bodies localized to the apical membrane in ciliated control MCCs, while defects in both ciliation and basal body docking were evident in atp4a morphants (Fig. 2B). The MCC phenotype of atp4a morphants thus phenocopied the cellular phenotype of foxj1-deficient mammalian airway MCCs.

ATP4a is also required for Wnt/PCP-dependent polarization of cilia at the gastrocoel roof plate (Walentek et al., 2012). Dysregulation of Wnt/PCP signaling in MCCs leads to defects in the formation of the apical actin meshwork, basal body docking and ciliation, but in addition it is also required for the uniform alignment of individual basal bodies in MCCs (Mitchell et al., 2009; Park et al., 2008). We therefore analyzed basal body directionality in atp4aMO injected MCCs using centrin4-RFP and clamp-GFP constructs (Park et al., 2008; Fig. 2C). Uniformly aligned basal bodies were found in control specimens, while the alignment was randomized in ATP4a-deficient MCCs (Fig 2C; Fig. S4), suggesting that ATP4a regulates Wnt/PCP-dependent aspects of MCC morphogenesis, in addition to Foxj1-dependent processes.

Next, we asked whether ATP4's effects on foxj1 expression and ciliation in MCCs were caused by interference with Wnt/β-catenin signaling (Fig. 3), as it was shown in the context of LR-axis formation (Walentek et al., 2012). To this end, atp4aMO was co-injected with DNA constructs encoding ATP4a (Fig. 3C, C′), β-catenin (Fig. 3D, D′) or Foxj1 (Fig. 3E, E ′). DNA injections were chosen to prevent early Wnt-dependent effects such as secondary axis induction, and have previously been effective in such rescues as well as for overexpression (Song et al., 2014; Walentek et al., 2012, 2013, 2014). While full ciliation failed in atp4a morphants, the overall morphology of the skin epidermis was remarkably normal; large goblet cells and smaller intercalating cells were clearly visible (Fig. 3A, B) and the total number of tubulin-positive cells (containing cilia or apically enriched tubulin) was not significantly different between atp4a morphants and uninjected control embryos (Fig. 3F, right panel). Either of the DNA constructs was sufficient to partially rescue skin ciliation ($p<0.001$; Fig. 3F) and to restore ciliary motility in atp4a morphants (cf. supplementary material Movie1).

In addition to rescue experiments using DNA co-injection, the specificity of the atp4aMO was confirmed by a) atp4a knockdown using a second non-overlapping translation blocking MO (atp4aMO-2; Fig. S5G–H, K), b) a splice-site MO (atp4a-SplMO; Fig. S5I–K) targeting the second exon/intron boundary of atp4a pre-mRNA, which lead to atp4a intron 2 retention as confirmed by PCR (see Fig. 4 in Walentek et al. 2015), and c) specific pharmacological inhibition of ATP4 using SCH28080 (Fig. S5A–B, K; Walentek et al, 2012). Each of these treatments caused MCC ciliation defects comparable to atp4aMO injections, without significant decrease in tubulin enriched epidermal cells (Fig. S5K).

In addition to partial or full loss of MCC ciliation, we observed increased numbers of MCCs with a relatively small apical surface in SCH28080, atp4aMO-2 and atp4aSplMO treated specimens, which likely contributes to loss of mucociliary clearance. In contrast to MO-mediated knockdown, pharmacological inhibition of ATP4 by SCH28080 also caused a frequent enlargement of epidermal cells, indicating additional defects in epithelial morphogenesis or homeostasis.

Together these data indicated that ATP4-mediated Wnt/β-catenin signaling was required for foxj1 expression and maturation of MCCs, without compromising cell type specification or intercalation of MCCs.

Wnt/β–catenin signaling acts downstream of Notch/Delta-mediated cell type specification on foxj1 expression

Activation of Notch signaling prevents MCC and ISC specification, while inhibition of Notch signaling increases the number of MCCs and ISCs, (Deblandre et al., 1999). To integrate canonical Wnt signaling into the pathway of MCC development, we investigated the interaction of Wnt and Notch signaling. Inhibition of Notch signaling by injection of a dominant-negative mutant of suppressor of hairless (Su(H)-DBM; Deblandre et al., 1999) increased foxj1 expression in the skin ectoderm in comparison to the uninjected contralateral side ($p<0.001$; Fig. 4A–B, E), as previously described for other markers of ciliated cells (Deblandre et al., 1999; Ossipova et al., 2007; Stubbs et al., 2012; Tan et al., 2013). In contrast, injection of both atp4aMO and Su(H)-DBM led to a marked decrease of foxj1 expression ($p<0.001$; Fig. 4C, E). Restoring Wnt signaling by injection of β-catenin DNA reversed the effect on foxj1 expression, i.e. triple injected specimens revealed an upregulation of foxj1 ($p<0.001$; Fig. 4D, E), similar to inhibition of Notch signaling alone (cf. Fig. 4B, E). Injection of β-catenin DNA alone did not significantly alter MCC ciliation or number of MCCs (Fig. S6A–C), in agreement with previously published work, in which gain of canonical Wnt signaling did not increase the number of α-tubulin expressing cells in the Xenopus embryonic epidermis (Ossipova et al. 2012).

In summary, these experiments demonstrated that Wnt/β-catenin signaling acts permissively downstream of Notch-mediated cell type specification and was required for MCC foxj1 expression.

ATP4-dependent Wnt/β–catenin regulates serotonin signaling in the ciliated epidermis

We have recently shown that small secretory cells (SSCs) synthesize and secrete serotonin, which regulates beating of MCC cilia via serotonin receptor type 3 (5-Htr3; Walentek et al 2014). Furthermore, SSCs are required to protect the embryo from bacterial infection (Dubaissi et al., 2014). In atp4a morphants the number of SSCs and foxa1 expression were greatly reduced (Fig. 1A–C; Fig. S2B; Fig. S3B). To further test how SSCs were affected by ATP4a loss-of-function, we examined serotonin deposition (Walentek et al. 2014). Serotonin was found in vesicle-like structures in control embryos, and these were lost in atp4a morphants ($p<0.001$; Fig. 5A–B, E). Co-injection of atp4a or β–catenin DNA restored serotonin in SSCs ($p<0.001$; Fig. 5C–E), indicating that Wnt signaling regulates SSCs in the epidermis. tph1, which is expressed in SSCs (Fig. 5F, F′; Walentek et al. 2014), was also

downregulated in atp4a morphants (Fig. 5G, G′). Co-injection of atp4a DNA rescued expression of tph1 to about control levels (Fig. 5H, H′).

These data confirmed our findings on foxa1/tph1 downregulation and showed that ATP4a-dependent Wnt signaling was also required for SSC function in the embryonic epidermis.

Endogenous Wnt/β–catenin signaling is required for MCC and SSC development in the embryonic epidermis

In addition to canonical Wnt signaling, ATP4a is also required for Wnt/PCP signaling during Xenopus LR development (Walentek et al., 2012). Certain aspects of the MCC phenotype in atp4a morphants, i.e. apical actin formation, basal body docking and polarized alignment of basal bodies (Fig. 2), could be in part caused by defects in Wnt/PCP signaling as well. In order to dissect the impact of the two Wnt pathway branches on the ciliated epidermis, we inhibited canonical Wnt/β-catenin signaling by overexpression of dickkopf (dkk) mRNA (Niehrs, 2006). This inhibition caused defects in MCC ciliation ($p<0.001$; Fig. 6A–C) and SSC serotonin deposition ($p<0.001$; Fig. 6A–C), similar to ATP4a loss-of-function (cf. Fig. 3,5). MCCs presented fewer and shorter cilia at their apical surfaces and the number of cells positive for serotonin staining was strongly decreased (Fig. 6A′, A″, B′, B″ and C). Importantly, defects in MCC ciliation in dkk injected specimens were less severe compared to atp4a morphants and apical actin formation was less affected. We therefore suggest that the MCC phenotype in atp4a morphants was the result of combined deficiencies in Wnt/β-catenin and Wnt/PCP signaling.

We also observed a consistent increase in the number of MCCs in dkk injected embryos (Fig. 6C). Although the magnitude of this effect was not statistically significant ($p=0.07$), it might indicate additional roles of Wnt/β-catenin signaling in MCC cell fate specification. To reveal subtle differences between the atp4aMO and dkk phenotypes, we analyzed transcription of mucociliary genes by qPCR (Fig. S3). In dkk injected specimens, we found similar changes in gene expression to atp4aMO injected animal caps (Fig. S3), although in contrast to atp4aMO, mci expression was increased ($p=0.06$) during early and late cell type specification stages (Fig. S3A) and foxi1 expression was moderately affected in late cell fate specification and intercalation stages (Fig. S3C). myb ($p>0.05$), foxj1 ($p<0.01$/$p<0.001$), foxa1 ($p<0.05$/$p<0.001$) and tph1 ($p<0.001$) expression was persistently stronger affected in atp4a morphants than after dkk injection (Fig. S3).

Taken together, these data support a requirement for ATP4a-dependent Wnt/β-catenin signaling in mucociliary gene expression, and strongly indicates that ATP4 acts through Wnt/β-catenin signaling on the regulation of foxj1 and foxa1 expression in MCC ciliation and SSC cell fate specification, respectively.

Recent work reported an additional requirement for Wnt/β-catenin signaling during specification of the deep ectodermal cell layer (Huang and Niehrs, 2014), although our β-catenin DNA overexpression data (Fig. S6) and previous reports by another group (Ossipova et al. 2012) did not reveal any influence of β-catenin injections on the number of epidermal MCCs. Our atp4a DNA injections may not suffice to induce an early response to canonical Wnt signaling and, thus, not affect the specification process of deep ectodermal cells.

Therefore, we injected β-catenin mRNA targeted to the epidermal ectoderm at concentrations that were sufficient to induce secondary axis formation upon injection into the ventral marginal zone of 4-cell stage embryos (not shown). Overexpression of β-catenin mRNA (β-cat. RNA; Fig. S7) did not consistently lead to increased numbers of MCCs or SSCs in the epidermis at stage 32 (Fig. S7C–D), although it is noteworthy that in two out of twelve specimens a massive increase in MCCs occurred, indicating a potentially more complex relationship between canonical Wnt signaling and MCC specification.

In summary, our data revealed a developmental requirement for ATP4a-dependent Wnt/β-catenin signaling during Foxj1-mediated motile ciliogenesis and Foxa1-mediated specification of SSCs in the mucociliary epidermis of Xenopus embryos.

Pharmacological inhibition of ATP4 in the mature mucociliary epidermis decreases the number of MCC and results in loss of extracellular fluid flow

Our experimental results argue strongly for a role of ATP4 during development of the Xenopus mucociliary epidermis, thereby suggesting a potential role for ATP4 in mucociliary clearance in the mammalian airway epithelium as well. In contrast to our early interventions in the embryo, PPIs are administered to adult patients after development of the airway epithelium. In order to address how pharmacological inhibition of ATP4 in mature mucociliary epithelia could influence mucociliary clearance, we performed experiments in which SCH28080 was applied at different stages of epidermal development and function. Both MCC ciliation and serotonin deposition were analyzed as readout (Fig. S5A–F, K; Fig. 7). When applied early (stage 5–30), SCH28080 incubations had essentially the same effects on MCCs and SSCs as MO-mediated knockdown of atp4a (Fig. S5A–B, G–J, K; Fig. 3), while later application of SCH28080 during epidermal development, starting at stages 12 or 22, had statistically significant but less pronounced effects on both MCC ciliation ($p<0.001$; Fig. S5C–D, E–F, K) and number of SSCs ($p<0.01/p>0.05$; Fig. S5C–D, E–F, K). These data indicated that ATP4 plays mainly a developmental role in MCC ciliation and specification of SSCs in the embryonic epidermis. In line with this assumption, SCH28080-mediated inhibition of ATP4 starting at stage 29, i.e. when functional MCCs and SSCs were already present, did not significantly affect ciliation or serotonin deposition in MCCs and SSCs, respectively (Fig. S5K; Fig. 7A–B). Nevertheless, a quantitative analysis of extracellular fluid flow (Walentek et al., 2014) revealed significantly reduced velocities of automatically tracked fluorescent beads at stage 35 in tadpoles treated with SCH28080 from stage 29 onwards ($p<0.05$; Fig. 7E). Prolonged incubation of tadpoles in SCH28080-containing media until stage 41 further decreased extracellular fluid flow velocities, resulting in an almost complete loss of mucociliary clearance ($p<0.001$; Fig. 7E). Interestingly, tadpoles treated with SCH28080 from stage 30–41 (~72h) displayed a massive loss of MCCs (ciliated MCCs as well as tubulin-enriched cells) in the epithelium, while serotonin-containing SSCs were not affected (Fig. 7C–D). Analysis of epidermal morphology using high-resolution confocal microscopy further revealed loss of cells containing a MCC-specific apical actin meshwork, apical enlargement of ISC-like cells as well as SSCs, and accumulations of actin at cell junctions (Fig. 7F–G). This phenotype suggested that MCCs were lost in the epithelium, leading to a decrease in apical surface

tension and, therefore, allowing other intercalating cell types to expand their apical surface area.

Finally, we analyzed how this late and prolonged SCH28080 incubation affected foxj1 expression in the epidermis. While epidermal foxj1 expression in control embryos at stage 40 was rather weak, strong expression was found in SCH28080 treated tadpoles, including a moderate increase in foxj1-positive cells (Fig. 7H–I; quantification not shown). These findings suggested that foxj1 expression might be upregulated in SCH28080 treated embryos in an attempt to regenerate and supply the epidermis with newly specified MCCs. Thus, withdrawal of the drug may lead to rapid recovery of mucociliary function.

In conclusion, inhibition of ATP4 during mucociliary development affected Foxj1-mediated ciliation in MCCs as well as Foxa1-dependent SSC specification and serotonin signaling. Inhibition of ATP4 function in established mucociliary epithelia led to a specific loss of MCCs from the epithelium, without reduction of foxj1 expression or loss of SSCs, consequently affecting mucociliary clearance at the embryonic epidermis, possibly by a Foxj1/Foxa1-independent mechanism.

Discussion

Understanding the complex process of formation and function of mucociliary epithelia is important in order to gain insight into the pathophysiological changes underlying human airway diseases. Spatiotemporal control of multiciliated and secretory cell specification, morphogenesis and function is a prerequisite for epithelial barrier function and mucus clearance in mucociliary epithelia, including the mammalian airways. A wide range of human syndromes, collectively addressed as ciliopathies, arise in patients when formation and function of motile cilia are disturbed. Syndromes include - among others - primary cilia dyskinesia (PCD), chronic obstructive pulmonary disease (COPD) and Meckel-Gruber syndrome, which are all associated with dysfunction of respiratory epithelia and increased rates of airway infections (Bergmann, 2012; Fliegauf et al., 2007; Mall, 2008; Zariwala et al., 2011). Similarly, defects in secretory cell function affect the ability of the airways to withstand pathogens (Kim and Criner, 2013; Mall, 2008; Wang et al., 2014).

We have used the Xenopus epidermis as a proxy to understand the effects of manipulating ATP4a on the spatiotemporal control of multiciliated and secretory cell specification, morphogenesis and function. Our data indicate that loss of ATP4 function leads to defects in Wnt signaling and, subsequently, impaired ciliogenesis of motile cilia throughout Xenopus development, i.e. the gastrocoel roof plate (Walentek et al., 2012), the neuroectoderm (cf. Fig. 1,2 in Walentek et al., 2015) and the mucociliary epidermis (Fig. 3,6). A prominent feature of the atp4a morphant phenotype was reduced foxj1 expression (Fig. 1, S2). Defects in multiciliated cells (MCCs) resulting from atp4a knockdown largely resembled loss of Foxj1 function, i.e. impaired ciliogenesis, due to basal body docking defects and lack of apical actin meshwork formation (Fig. 2; Gomperts et al., 2004). Additionally, atp4a morphants showed decreased levels of myb expression, while mci was unaffected (Fig. S3). Thus, while foxj1 and myb dependent ciliogenesis was disrupted, the specification of cells, marked by mci, was normal.

MCI and Myb can both induce basal body duplication and multiciliogenesis (Stubbs et al., 2012; Tan et al., 2013), while Foxj1 is necessary for ciliary motility in mono- and multiciliated cells (Stubbs et al., 2008; Yu et al., 2008). myb expression was downregulated and basal body numbers appeared slightly reduced in atp4a morphant MCCs (Fig. 2, S3). Although the aggregation of basal bodies (Fig. 2B, C; Fig. S4), which is often associated with basal body docking defects, prevented accurate quantification, it is possible that the effect on myb expression could lead to impaired basal body multiplication in addition to Foxj1-dependent motile ciliogenesis defects. We have previously shown that ATP4a was not only required for Wnt/β-catenin-dependent aspects of Xenopus development, but was equally important for Wnt/PCP-dependent processes (Walentek et al., 2012). We observed misalignment of basal bodies in MCCs of atp4a morphants (Fig. 2, S4), a feature commonly seen after dysregulation of the Wnt/PCP pathway (Mitchell et al., 2009; Park et al., 2008). Thus it is likely that ATP4 acts through Wnt/PCP signaling in MCCs as well, which could reinforce the cellular phenotype at the level of docking and alignment of basal bodies, as well as ciliation and apical actin organization. We conclude from these experiments that foxj1 downregulation comprised the major phenotype in ATP4a-deficient MCCs, likely accompanied by aspects which originate from defective myb expression and inhibition of Wnt/PCP signaling.

In zebrafish, foxj1 is directly regulated by canonical Wnt signaling (Caron et al., 2012). In Xenopus, ATP4a-dependent Wnt/β-catenin was required for foxj1 expression in the gastrocoel roof plate (Walentek et al., 2012), the epidermis and the neuroectoderm (Walentek et al., 2015), suggesting that foxj1 might be regulated by β-catenin throughout the vertebrates. Expression of Wnt pathway components (e.g. wnt4 and axin2) was shown to increase during air liquid interphase (ALI) culture of human airway epithelial cells (Ross et al., 2007) and multiple roles for canonical Wnt signaling have been proposed during mammalian lung development, in airway stem cells and disease (Hashimoto et al., 2012; Pongracz and Stockley, 2006; Sharma et al., 2010). As the roles of Notch, MCI, Myb and Foxj1 are functionally conserved between the Xenopus skin and mammalian airway epithelia, it is likely that a Wnt-dependent gene regulatory network is also present in the human respiratory tract.

Importantly, we found another process during development of the mucociliary epithelium to be under the control of ATP4 and canonical Wnt, namely the specification and function of small secretory cells (SSCs). Loss of ATP4a through pharmacological inhibition, or MO-mediated knockdown, or inhibition of canonical Wnt signaling by dkk injection decreased serotonin synthesis in SSCs (Fig. 5,6). Furthermore, SSC cell fate specification was likely affected by atp4aMO and dkk injection, because foxa1 expression was reduced by both treatments (Fig. 1, S2B, S3B). Serotonin is a known regulator of ciliary beat frequency in MCCs of mucociliary epithelia, including the human respiratory tract (Bayer et al., 2007; Doran, 2004; Katow et al., 2007; König et al., 2009; Walentek et al., 2014). Additionally, SSCs were required in Xenopus to regulate mucus composition and to prevent bacterial infection (Dubaissi et al., 2014), implicating that loss of SSCs might have additional consequences on other secretory cell types in the epidermis.

In addition to its developmental function as a permissive factor for Wnt signaling activation, ATP4 seems to play an additional role in homeostasis and function of mature MCCs. Decrease in MCCs in the epidermis after late treatment with the specific ATP4 inhibitor SCH28080 and expansion of the apical surfaces of neighboring intercalating cells indicate that MCCs were lost from the epithelium (Fig. 7). Loss of MCCs in this context might possibly be due to over-acidification of the cytoplasm and subsequent apoptosis, a mechanism previously described in human gastric cancer cell lines treated with various PPIs (Yeo et al., 2004). It will be interesting to investigate whether inhibition of ATP4 in mature MCCs leads to intracellular acidification, which would activate pH-dependent Caspase function and subsequently lead to cell-type specific apoptosis.

Several atp4a knock-out strains were generated over the past years. Analysis of these mice revealed phenotypes related to abnormal gastric function, i.e. gastric ciliated and mucocystic mataplasia (Judd et al., 2005; Spicer et al., 2000), and iron-deficiency (Krieg et al., 2011). Additionally, ATP4a loss of function affects ion homeostasis in the kidney (Greenlee et al., 2011; Lynch et al., 2008). Apart from these reports, we lack further knowledge on extragastric functions of ATP4a in the mouse. It should be mentioned that atp4a knock-out mice were not reported to be more susceptible to airway infections, but a specific function of ATP4a in the mouse airways was not investigated to date and housing of transgenic mice in pathogen-free facilities might have prevented such infections. Furthermore, atp4a knock-out mice do not show developmental defects associated with ATP4a loss of function in other species, e.g. left-right axis specification defects (Walentek et al., 2012), indicating either redundancy or that the developmental function of ATP4a was lost in mice during evolution. This suggests that the mouse might not be the best model to investigate all extragastric functions of ATP4a related to human development and disease. Taken together, the data presented here supports the presence of a general ATP4/canonical Wnt/Foxj1 module for the regulation of ciliation and mucociliary function in the frog Xenopus. Our findings argue for several roles of ATP4-dependent Wnt signaling during mucociliary development and clearance. The experimental results suggest two potential mechanisms how proton pump inhibitor treatment could act on the human airways and result in an increased susceptibility for acquired infections: airway clearance could be either affected by PPI-mediated down-regulation of ATP4-dependent Wnt signaling, or due to negative effects on mature MCCs. This strongly suggests that PPI-associated pneumonia in human patients might, at least in part, be linked to dysfunction of airway epithelia and highlights the Xenopus epidermis as an important model for the study of mucociliary epithelia.

Materials and methods

Ethics statement

All animals were treated according to the German regulations and laws for care and handling of research animals, and experimental manipulations according to §6, article 1, sentence 2, no. 4 of the animal protection act were approved by the Regional Government Stuttgart, Germany (Vorhaben A 365/10 ZO “Molekulare Embryologie”).

This work was also done with approval of University of California, Berkeley's Animal Care and Use Committee. University of California, Berkeley's assurance number is A3084-01, and is on file at the National Institutes of Health Office of Laboratory Animal Welfare.

Statistical evaluation of results

Statistical evaluation of experiments represented by bar graphs was performed using chi-square tests (http://www.physics.csbsju.edu/stats/contingency.html). Statistics of experiments represented by box plots were calculated by Wilcoxon sum of ranks (Mann-Whitney) tests (http://www.fon.hum.uva.nl/Service/Statistics/Wilcoxon_Test.html). Significance of qRT-PCR results was determined using Student's T-test (http://www.physics.csbsju.edu/stats/t-test.html). S.E.M. was calculated using http://www.miniwebtool.com/standard-error-calculator/.

Manipulation of embryos

Embryos were injected at the two- to four-cell stage using a Harvard Apparatus or Picospritzer setup in 1x modified Barth's solution (MBSH) with 4% Ficoll (BioChemica) and transferred to 0.1x MBSH 15 min after injection. atp4aMO (5′-GTCATATTGTTCCTTTTTCCC CATC-3′) 1pmol, atp4aMO-2 (5′-CTCTCTCCATCTCCACCGAGAACAT-3′) 1pmol, atp4aSplMO (5′-CCCCCCCCCCCATTTCTTACAATGT-3′) 3pmol or CoMO (random control morpholino oligonucleotide; Gene Tools) 1pmol were injected. Drop size was calibrated to about 7–8 nl per injection. Rhodamine-B or Cascade-blue dextran (0.5–1.0 mg/ml; Molecular Probes) were co-injected and used as lineage tracer. DNAs were purified using the PureYield Plasmid Midiprep kit (Promega) and diluted to a concentration of 0.5 ng/µl (foxj1-CS2^{+}; Stubbs et al., 2008), 1 ng/µl (ATP4a-CS2^{+}MT; Walentek et al., 2012) and β-cat-gfp-CS2^{+}; (Miller and Moon, 1997). Synthesis of mRNAs used the Ambion message machine kit and mRNAs were diluted to the following concentrations: Su(H)-DBM and Notch-ICD 150ng/µl (Deblandre et al., 1999); dkk 5ng/µl (Glinka et al., 1998); sas6-gfp 10ng/µl (Klos Dehring et al., 2013); centrin-gfp and clamp-gfp 50ng/µl (Park et al., 2008). SCH28080 (Sigma-Adrich; solvent: DMSO; concentration: 100µM) incubations were performed according to standard procedures on embryos treated with Proteinase K (as described; Sive et al., 2000) in order to permeabilize the fertilization membrane (in case of early incubation experiments). Proteinase K-treated embryos incubated with corresponding concentrations of DMSO were used as controls.

Quantitative RT-PCR

qRT-PCR experiments were performed in three biological experiments and three technical replicates per experiment. cDNAs were synthesized using iScript reverse transcription supermix (BioRad) from total RNA extracts from 15 animal caps per condition and time point. The following qPCR primers were used:

foxj1: For 5′-CCAGTGATAGCAAAAGAGGT-3′, Rev 5′-GCCATGTTCTCCTAATGGAT-3′;

mci: For 5′-AATCAAAAGCATCTGTC-3′, Rev 5′-TTTCTTAGAGATTTCCCGCA-3′;

myb: For 5′-CAGAATGCTTCATACCCTGT-3′, Rev: 5′-CAGTAGTTCTTGCTTCTGTG-3′;

foxa1: For 5′-GGAGCAACTATTACCAGGAC-3′, Rev: 5′-ATGGGATTCATAGTCATGTAGG-3′;

foxi1: For 5′-TACCAAGAGATGAAGATGATC-3′, Rev: 5′-CTTGTCAGAAGATAACTGTCCA-3′;

tph1: For 5′-CTGGTTTCAAGGACAATGTG-3′, Rev: 5′-GGCAGGTTCTTTAGGTACTC-3′;

ef1a: For 5′-CCCTGCTGGAAGCTCTTGAC-3′, Rev 5′-GGACACCAGTCTCCACACGA-3′;

odc: For 5′-GGGCTGGATCGTATCGTAGA-3′, Rev 5′-TGCCAGTGTGGTCTTGACAT-3′.

Reactions were performed on a BioRad CFX96 Real-Time System C1000 Touch using SsoAdvanced SYBR Green Supermix (Biorad). Average values from ef1a and odc reactions were used for normalization. The expression levels depicted were calculated as fold expression relative to stage 10 uninjected control.

Whole-mount in situ hybridization

Embryos were fixed in MEMFA for 1–2 hrs and processed following standard protocols. Digoxigenin-labeled (Roche) RNA probes (atp4a and foxj1, Walentek et al., 2012; atp6V1E1 probe was generated according to NM_001086298; tph1; Walentek et al., 2014; foxi1, (Quigley et al., 2011); foxa1; (Hayes et al., 2007) were prepared from linearized plasmids using SP6, T3, or T7 RNA polymerase (Promega). In situ hybridization was conducted following standard procedures. In some experiments (Fig. 1C) embryos were bleached after in situ hybridization according to standard procedures (Sive et al., 2000).

Immunohistochemistry and scanning electron microscopy

Immunohistochemistry followed standard protocols (Sive et al., 2000), using antibodies specific for acetylated-α-tubulin (mouse, 1:700; Sigma), ATP4a (1:500; Walentek et al., 2012), anti-mouse Cy3 (sheep, 1:250; Sigma); serotonin (rabbit, 1:500; Merck), anti-rabbit Alexa-555 (1:250; Invitrogen), anti-mouse Alexa-555 (1:250; Invitrogen), anti-mouse Alexa-405 (1:250; Invitrogen). Cell boundaries were visualized by Alexa 488-conjugated phalloidin (Invitrogen), which stained the actin cytoskeleton. Imaging was performed on a Zeiss LSM710. Lateral projections of confocal z-scans were computed using Zeiss Zen software. Maximum intensity projections of confocal z-scans were computed using ImageJ (Schindelin et al., 2012). Scanning electron microscopy was as previously described (Beyer et al., 2012).

Imaging of fluid flow

For imaging of skin flow in supplementary material Movie1, stage 29 embryos were anesthetized with benzocaine (Sigma) and exposed to fluorescent latex beads (FluoSpheres® carboxylate-modified microspheres, 0.5 μm, yellow-green fluorescence [505/515], 2%

solids, Life Technologies; diluted to 0.04% in 0.1 x MBSH) in a sealed flow chamber. Time-lapse movies (20 sec) were recorded using epifluorescent illumination at 10x magnification on a Zeiss Axioskop 2 microscope and processed in ImageJ.

For imaging of skin flow at later stages (supplementary material Movie2), stage 35 or stage 41 embryos treated with either DMSO (1%) or SCH28080 (100μM) were anesthetized and exposed to latex beads (FluoSpheres® carboxylate-modified microspheres, 0.5 μm, red fluorescence [580/605], 2% solids, Life Technologies; diluted to 0.04% in 0.1 x MBSH) in a sealed flow chamber. Time-lapse movies (10 sec/50 frames per sec) were recorded using epifluorescent illumination at 20x magnification on a Zeiss Axioskop 2 microscope in combination with a high-speed GX-1Memrecam camera (NACImage Technology) and processed in ImageJ. Particle linking and quantification of extracellular fluid flow velocities was performed as previously described cf. Walentek et al. (2012, 2014).

Supplementary Material

Refer to Web version on PubMed Central for supplementary material.

Acknowledgments

Helpful discussions and sharing of reagents are gratefully acknowledged: H. Fischer, K. Geehring, B. Illek, C. Kintner, P. Lishko, T. Machen, B. Mitchell, N. Papalopulu, I. Schneider, B. Ulmer, and J. Wallingford. We thank S. Bogusch, A. Schäfer and I. Sun for expert technical support.

Funding

Work in the Blum lab was supported by a grant from the Deutsche Forschungsgemeinschaft (BL-285/9) to MB. Xenopus work in the Harland lab was supported by the NIH (GM42341). PW and TB were recipients of Ph.D. fellowships from the Landesgraduiertenförderung Baden-Württemberg. PW was also supported by a postdoctoral fellowship from the Deutsche Forschungsgemeinschaft (Wa 3365/1-1). CH and KF are indebted to the Baden-Württemberg Stiftung for the financial support of their research by the Eliteprogramme for Postdocs. KF was supported by a Margarete-von-Wrangell fellowship, funded by the European Social Fund and by the Ministry Of Science, Research and the Arts in Baden-Württemberg.

References

Altman KW, Waltonen JD, Tarjan G, Radosevich Ja, Haines GK. Human lung mucous glands manifest evidence of the H+/K+-ATPase proton pump. Ann Otol Rhinol Laryngol. 2007; 116:229–34. [PubMed: 17419528]

Avasthi P, Marshall WF. Stages of ciliogenesis and regulation of ciliary length. Differentiation. 2012; 83:S30–42.10.1016/j.diff.2011.11.015 [PubMed: 22178116]

Bayer H, Müller T, Myrtek D, Sorichter S, Ziegenhagen M, Norgauer J, Zissel G, Idzko M. Serotoninergic receptors on human airway epithelial cells. Am J Respir Cell Mol Biol. 2007; 36:85–93.10.1165/rcmb.2006-0151OC [PubMed: 16873768]

Bergmann C. Educational paper: ciliopathies. Eur J Pediatr. 2012; 171:1285–300.10.1007/s00431-011-1553-z [PubMed: 21898032]

Beyer T, Danilchik M, Thumberger T, Vick P, Tisler M, Schneider I, Bogusch S, Andre P, Ulmer B, Walentek P, Niesler B, Blum M, Schweickert A. Serotonin Signaling Is Required for Wnt-Dependent GRP Specification and Leftward Flow in Xenopus. Curr Biol. 2012; 22:1–7.10.1016/j.cub.2011.11.027 [PubMed: 22197242]

Caron A, Xu X, Lin X. Wnt/β-catenin signaling directly regulates Foxj1 expression and ciliogenesis in zebrafish Kupffer's vesicle. Development. 2012; 139:514–24.10.1242/dev.071746 [PubMed: 22190638]

Crystal RG, Randell SH, Engelhardt JF, Voynow J, Sunday ME. Airway epithelial cells: current concepts and challenges. Proc Am Thorac Soc. 2008; 5:772–7.10.1513/pats.200805-041HR [PubMed: 18757316]

De Jager CPC, Wever PC, Gemen EFa, van Oijen MGH, van Gageldonk-Lafeber aB, Siersema PD, Kusters GCM, Laheij RJF. Proton pump inhibitor therapy predisposes to community-acquired Streptococcus pneumoniae pneumonia. Aliment Pharmacol Ther. 2012; 36:941–9.10.1111/apt.12069 [PubMed: 23034135]

Deblandre GA, Wettstein DA, Koyano-Nakagawa N, Kintner C. A two-step mechanism generates the spacing pattern of the ciliated cells in the skin of Xenopus embryos. Development. 1999; 126:4715–4728. [PubMed: 10518489]

Doran SA. Effect of serotonin on ciliary beating and intracellular calcium concentration in identified populations of embryonic ciliary cells. J Exp Biol. 2004; 207:1415–1429.10.1242/jeb.00924 [PubMed: 15010492]

Dubaissi E, Papalopulu N. Embryonic frog epidermis: a model for the study of cell-cell interactions in the development of mucociliary disease. Dis Model Mech. 2011; 192:179–192.10.1242/dmm.006494 [PubMed: 21183475]

Dubaissi E, Rousseau K, Lea R, Soto X, Nardeosingh S, Schweickert A, Amaya E, Thornton DJ, Papalopulu N. A secretory cell type develops alongside multiciliated cells, ionocytes and goblet cells, and provides a protective, anti-infective function in the frog embryonic mucociliary epidermis. Development. 2014; 141:1514–25.10.1242/dev.102426 [PubMed: 24598166]

Fischer H, Widdicombe J. Mechanisms of acid and base secretion by the airway epithelium. J Membr Biol. 2006; 211:139–150.10.1007/s00232-006-0861-0.Mechanisms [PubMed: 17091214]

Fliegauf M, Benzing T, Omran H. When cilia go bad: cilia defects and ciliopathies. Nat Rev Mol Cell Biol. 2007; 8:880–893.10.1038/nrm2278 [PubMed: 17955020]

Fohl AL, Regal RE. Proton pump inhibitor-associated pneumonia: Not a breath of fresh air after all? World J Gastrointest Pharmacol Ther. 2011; 2:17–26.10.4292/wjgpt.v2.i3.17 [PubMed: 21731913]

Glinka A, Wu W, Delius H, Monaghan AP, Blumenstock C, Niehrs C. Dickkopf-1 is a member of a new family of secreted proteins and functions in head induction. Nature. 1998; 391:357–62.10.1038/34848 [PubMed: 9450748]

Gomperts BN, Gong-Cooper X, Hackett BP. Foxj1 regulates basal body anchoring to the cytoskeleton of ciliated pulmonary epithelial cells. J Cell Sci. 2004; 117:1329–37.10.1242/jcs.00978 [PubMed: 14996907]

Greenlee MM, Lynch IJ, Cain BD, Wingo CS. Mineralocorticoids stimulate the activity and expression of renal H+, K+-ATPases. J Am Soc Nephrol. 2011; 22(1):49–58.10.1681/ASN.2010030311 [PubMed: 21164026]

Hashimoto S, Chen H, Que J, Brockway BL, Drake Ja, Snyder JC, Randell SH, Stripp BR. β-Catenin-SOX2 signaling regulates the fate of developing airway epithelium. J Cell Sci. 2012; 125:932–42.10.1242/jcs.092734 [PubMed: 22421361]

Hayes JM, Kim SK, Abitua PB, Park TJ, Herrington ER, Kitayama A, Grow MW, Ueno N, Wallingford JB. Identification of novel ciliogenesis factors using a new in vivo model for mucociliary epithelial development. Dev Biol. 2007; 312:115–30.10.1016/j.ydbio.2007.09.031 [PubMed: 17961536]

Herrmann M, Selige J, Raffael S, Sachs G, Brambilla A, Klein T. Systematic expression profiling of the gastric H+/K+ ATPase in human tissue. Scand J Gastroenterol. 2007; 42:1275–88.10.1080/00365520701405579 [PubMed: 17852870]

Herzig S, Doughty C, Lahoti S. Acid- Suppressive Medication Use in Acute Stroke and Hospital-Acquired Pneumonia. Ann …. 2014:1–28.

IMS Institute for healthcare informatics. The Use of Medicines in the United States: Review of 2010. 2011.

Jeffery PK, Li D. Airway mucosa: secretory cells, mucus and mucin genes. Eur Respir J. 1997; 10:1655–1662.10.1183/09031936.97.10071655 [PubMed: 9230262]

Jena AB, Sun E, Goldman DP. Confounding in the association of proton pump inhibitor use with risk of community-acquired pneumonia. J Gen Intern Med. 2013; 28:223–30.10.1007/s11606-012-2211-5 [PubMed: 22956446]

Judd LM, Andringa A, Rubio CA, Spicer Z, Shull GE, Miller ML. Gastric achlorhydria in H/K-ATPase-deficient (Atp4a(−/−)) mice causes severe hyperplasia, mucocystic metaplasia and upregulation of growth factors. J Gastroenterol Hepatol. 2005; 20(8):1266–78.10.1111/j.1400-1746.2005.03867.x [PubMed: 16048577]

Katow H, Yaguchi S, Kyozuka K. Serotonin stimulates [Ca2+]i elevation in ciliary ectodermal cells of echinoplutei through a serotonin receptor cell network in the blastocoel. J Exp Biol. 2007; 210:403–12.10.1242/jeb.02666 [PubMed: 17234609]

Kim V, Criner GJ. Chronic bronchitis and chronic obstructive pulmonary disease. Am J Respir Crit Care Med. 2013; 187:228–37.10.1164/rccm.201210-1843CI [PubMed: 23204254]

Klos Dehring, Da; Vladar, EK.; Werner, ME.; Mitchell, JW.; Hwang, P.; Mitchell, BJ. Deuterosome-mediated centriole biogenesis. Dev Cell. 2013; 27:103–12.10.1016/j.devcel.2013.08.021 [PubMed: 24075808]

König P, Krain B, Krasteva G, Kummer W. Serotonin increases cilia-driven particle transport via an acetylcholine-independent pathway in the mouse trachea. PLoS One. 2009; 4:e4938.10.1371/journal.pone.0004938 [PubMed: 19290057]

Krieg L, Milstein O, Krebs P, Xia Y, Beutler B, Du X. Mutation of the gastric hydrogen-potassium ATPase alpha subunit causes iron-deficiency anemia in mice. Blood. 2011; 118 (24):6418–25.10.1182/blood-2011-04-350082 [PubMed: 21976678]

Lynch IJ, Rudin A, Xia SL, Stow LR, Shull GE, Weiner ID, Cain BD, Wingo CS. Impaired acid secretion in cortical collecting duct intercalated cells from H-K-ATPase-deficient mice: role of Hkalpha isoforms. Am J Physiol Renal Physiol. 2008; 294 (3):F621–7.10.1152/ajprenal.00412.2007 [PubMed: 18057185]

Mall, Ma. Role of cilia, mucus, and airway surface liquid in mucociliary dysfunction: lessons from mouse models. J Aerosol Med Pulm Drug Deliv. 2008; 21:13–24.10.1089/jamp.2007.0659 [PubMed: 18518828]

Marshall WF. Basal Bodies: Platforms for Building Cilia. Curr Top Dev Biol. 2008; 85:1–22.10.1016/S0070-2153(08)00801-6 [PubMed: 19147000]

Marshall WF, Kintner C. Cilia Orientation and the Fluid Mechanics of Development. Curr Opin Cell Biol. 2008; 20:48–52.10.1016/j.ceb.2007.11.009.Cilia [PubMed: 18194854]

Miller JR, Moon RT. Analysis of the signaling activities of localization mutants of beta-catenin during axis specification in Xenopus. J Cell Biol. 1997; 139:229–43. [PubMed: 9314542]

Mitchell B, Jacobs R, Li J, Chien S, Kintner C. A positive feedback mechanism governs the polarity and motion of motile cilia. Nature. 2007; 447:97–101.10.1038/nature05771 [PubMed: 17450123]

Mitchell B, Stubbs JL, Huisman F, Taborek P, Yu C, Kintner C. Report The PCP Pathway Instructs the Planar Orientation of Ciliated Cells in the Xenopus Larval Skin. Curr Biol. 2009; 19:924–929.10.1016/j.cub.2009.04.018 [PubMed: 19427216]

Niehrs C. Function and biological roles of the Dickkopf family of Wnt modulators. Oncogene. 2006; 25:7469–81.10.1038/sj.onc.1210054 [PubMed: 17143291]

Ossipova O, Tabler J, Green JBA, Sokol SY. PAR1 specifies ciliated cells in vertebrate ectoderm downstream of aPKC. Development. 2007; 134:4297–306.10.1242/dev.009282 [PubMed: 17993468]

Park TJ, Mitchell BJ, Abitua PB, Kintner C, Wallingford JB. Dishevelled controls apical docking and planar polarization of basal bodies in ciliated epithelial cells. Nat Genet. 2008; 40:871–879.10.1038/ng.104 [PubMed: 18552847]

Pongracz JE, Stockley Ra. Wnt signalling in lung development and diseases. Respir Res. 2006; 7:15.10.1186/1465-9921-7-15 [PubMed: 16438732]

Proud D, Leigh R. Epithelial cells and airway diseases. Immunol Rev. 2011; 242:186–204.10.1111/j.1600-065X.2011.01033.x [PubMed: 21682746]

Quigley IK, Stubbs JL, Kintner C. Specification of ion transport cells in the Xenopus larval skin. Development. 2011; 714:705–714.10.1242/dev.055699 [PubMed: 21266406]

Ramsay EN, Pratt NL, Ryan P, Roughead EE. Proton pump inhibitors and the risk of pneumonia: a comparison of cohort and self-controlled case series designs. BMC Med Res Methodol. 2013; 13:82.10.1186/1471-2288-13-82 [PubMed: 23800078]

Reimer C. Safety of long-term PPI therapy. Best Pract Res Clin Gastroenterol. 2013; 27:443–54.10.1016/j.bpg.2013.06.001 [PubMed: 23998981]

Ross AJ, Dailey La, Brighton LE, Devlin RB. Transcriptional profiling of mucociliary differentiation in human airway epithelial cells. Am J Respir Cell Mol Biol. 2007; 37:169–85.10.1165/rcmb.2006-0466OC [PubMed: 17413031]

Sawaguchi, a; McDonald, KL.; Forte, JG. High-pressure Freezing of Isolated Gastric Glands Provides New Insight into the Fine Structure and Subcellular Localization of H+/K+-ATPase in Gastric Parietal Cells. J Histochem Cytochem. 2004; 52:77–86.10.1177/002215540405200108 [PubMed: 14688219]

Schindelin J, Arganda-Carreras I, Frise E, Kaynig V, Longair M, Pietzsch T, Preibisch S, Rueden C, Saalfeld S, Schmid B, Tinevez JY, White DJ, Hartenstein V, Eliceiri K, Tomancak P, Cardona A. Fiji: an open-source platform for biological-image analysis. Nat Methods. 2012; 9:676–82.10.1038/nmeth.2019 [PubMed: 22743772]

Sharma S, Tantisira K, Carey V, Murphy AJ, Lasky-Su J, Celedón JC, Lazarus R, Klanderman B, Rogers A, Soto-Quirós M, Avila L, Mariani T, Gaedigk R, Leeder S, Torday J, Warburton D, Raby B, Weiss ST. A role for Wnt signaling genes in the pathogenesis of impaired lung function in asthma. Am J Respir Crit Care Med. 2010; 181:328–36.10.1164/rccm.200907-1009OC [PubMed: 19926868]

Sheen E, Triadafilopoulos G. Adverse effects of long-term proton pump inhibitor therapy. Dig Dis Sci. 2011; 56:931–50.10.1007/s10620-010-1560-3 [PubMed: 21365243]

Shin JM, Munson K, Vagin O, Sachs G. The gastric HK-ATPase: structure, function, and inhibition. Eur J Physiol. 2009; 457:609–22.10.1007/s00424-008-0495-4

Shin JM, Sachs G. Dimerization of the gastric H+, K(+)-ATPase. J Biol Chem. 1996; 271:1904–8. [PubMed: 8567637]

Shin JM, Sachs G. Gastric H, K-ATPase as a drug target. Dig Dis Sci. 2006; 51:823–33.10.1007/s10620-005-9042-8 [PubMed: 16645899]

Sive, HL.; Grainger, RM.; Harland, RM. Early Development of Xenopus laevis. Cold Spring Harbor Laboratory Press; Cold Spring Harbor, NY, USA: 2000.

Song R, Walentek P, Sponer N, Klimke A, Lee JS, Dixon G, Harland R, Wan Y, Lishko P, Lize M, Kessel M, He L. miR-34/449 miRNAs are required for motile ciliogenesis by repressing cp110. Nature. 2014; 510:115–120.10.1038/nature13413 [PubMed: 24899310]

Spicer Z, Miller ML, Andringa A, Riddle TM, Duffy JJ, Doetschman T, Schull GE. Stomachs of Mice Lacking the Gastric H, K-ATPase a-Subunit Have Achlorhydria, Abnormal Parietal Cells, and Ciliated Metaplasia. The Journal of Biological Chemistry. 2000; 275 (28):21555–565.10.1074/jbc.M001558200 [PubMed: 10764766]

Stubbs JL, Davidson L, Keller R, Kintner C. Radial intercalation of ciliated cells during Xenopus skin development. Development. 2006; 133:2507–15.10.1242/dev.02417 [PubMed: 16728476]

Stubbs JL, Oishi I, Izpisúa Belmonte JC, Kintner C. The forkhead protein Foxj1 specifies node-like cilia in Xenopus and zebrafish embryos. Nat Genet. 2008; 40:1454–60.10.1038/ng.267 [PubMed: 19011629]

Stubbs JL, Vladar EK, Axelrod JD, Kintner C. Multicilin promotes centriole assembly and ciliogenesis during multiciliate cell differentiation. Nat Cell Biol. 2012; 14:1–10.10.1038/ncb2406

Tan FE, Vladar EK, Ma L, Fuentealba LC, Hoh R, Espinoza FH, Axelrod JD, Alvarez-buylla A, Stearns T, Kintner C, Krasnow MA. Myb promotes centriole amplification and later steps of the multiciliogenesis program. Development. 2013; 140:4277–86.10.1242/dev.094102 [PubMed: 24048590]

Walentek P, Beyer T, Thumberger T, Schweickert A, Blum M. ATP4a is required for Wnt-dependent Foxj1 expression and leftward flow in Xenopus left-right development. Cell Rep. 2012; 1:516–27.10.1016/j.celrep.2012.03.005 [PubMed: 22832275]

Walentek P, Bogusch S, Thumberger T, Vick P, Dubaissi E, Beyer T, Blum M, Schweickert A. A novel serotonin-secreting cell type regulates ciliary motility in the mucociliary epidermis of Xenopus tadpoles. Development. 2014; 141:1–8.10.1242/dev.102343

Walentek P, Hagenlocher C, Beyer T, Müller C, Feistel K, Schweickert A, Harland RM, Blum M. ATP4 and ciliation in the neuroectoderm and endoderm of Xenopus embryos and tadpoles. Data in Brief. 2015 in press.

Walentek P, Schneider I, Schweickert A, Blum M. Wnt11b is involved in cilia-mediated symmetry breakage during Xenopus left-right development. PLoS One. 2013; 8:e73646.10.1371/journal.pone.0073646 [PubMed: 24058481]

Wang SZ, Rosenberger CL, Bao YX, Stark JM, Harrod KS. Clara Cell Secretory Protein Modulates Lung Inflammatory and Immune Responses to Respiratory Syncytial Virus Infection. J Immunol. 2014; 171:1051–1060.10.4049/jimmunol.171.2.1051 [PubMed: 12847279]

Werner ME, Mitchell BJ. Understanding ciliated epithelia: the power of Xenopus. Genesis. 2012; 50:176–85.10.1002/dvg.20824 [PubMed: 22083727]

Werner ME, Mitchell BJ. Using Xenopus skin to study cilia development and function. Methods Enzymol. 2013; 525:191–217.10.1016/B978-0-12-397944-5.00010-9 [PubMed: 23522471]

Yeo M, Kim DK, Kim YB, Oh TY, Lee JE, Cho SW, Kim HC, Hahm KB. Selective Induction of Apoptosis with Proton Pump Inhibitor in Gastric Cancer Cells. Clinical Cancer Research. 2004; 10:8687–96.10.1158/1078-0432.CCR-04-1065 [PubMed: 15623654]

Yu X, Ng CP, Habacher H, Roy S. Foxj1 transcription factors are master regulators of the motile ciliogenic program. Nat Genet. 2008; 40:1445–53.10.1038/ng.263 [PubMed: 19011630]

Zariwala, Ma; Omran, H.; Ferkol, TW. The emerging genetics of primary ciliary dyskinesia. Proc Am Thorac Soc. 2011; 8:430–3.10.1513/pats.201103-023SD [PubMed: 21926394]

Highlights

- ATP4 is required for development and function of the ciliated epidermis
- ATP4 regulates canonical and non-canonical Wnt signaling during development
- Wnt signaling controls gene expression in multiciliated and small secretory cells
- ATP4-inhibitors cause loss of mucociliary clearance in mature ciliated epithelia

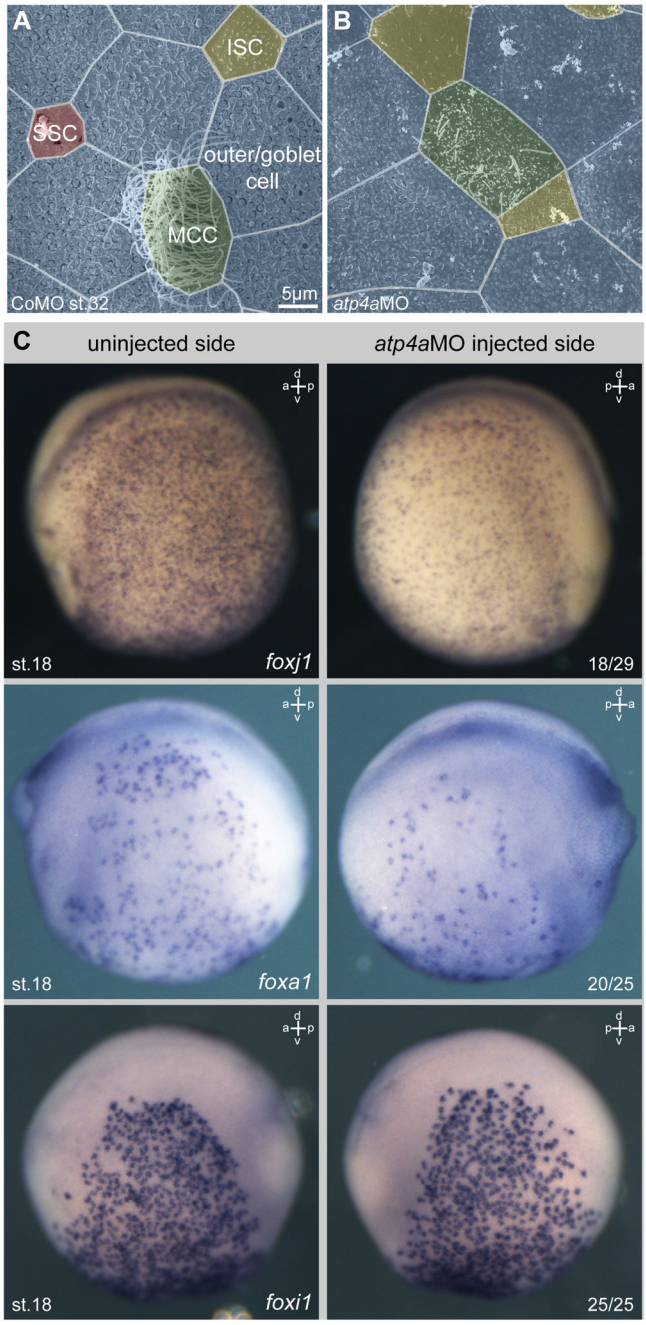

Fig. 1. ATP4 is required for normal development of the embryonic epidermis

(A–B) Morphological analysis of the embryonic epidermis at stage 32 in control morpholino oligonucleotide (CoMO) (A) and atp4aMO (B) injected specimens. Knockdown of atp4a lead to defects in ciliation of multiciliated cells (MCCs, green) and reduced numbers of small secretory cells (SSCs, red), but without obvious effects on ion secreting cells (ISCs, yellow) or outer/goblet cells (blue). (C) Knockdown of atp4a attenuated foxj1 and foxa1 expression, but not foxi1 expression in the skin epidermis. Embryos were unilaterally injected with atp4aMO at the four-cell stage and assayed for foxj1/foxa1/foxi1 expression by WMISH at stage 15. Correct targeting was confirmed by co-injection of lineage tracer.

Depicted embryos are derived from the same injected batch. Numbers in the right lower corner indicate frequency of phenotype.
a, anterior; d, dorsal; p, posterior; st., stage; v, ventral.

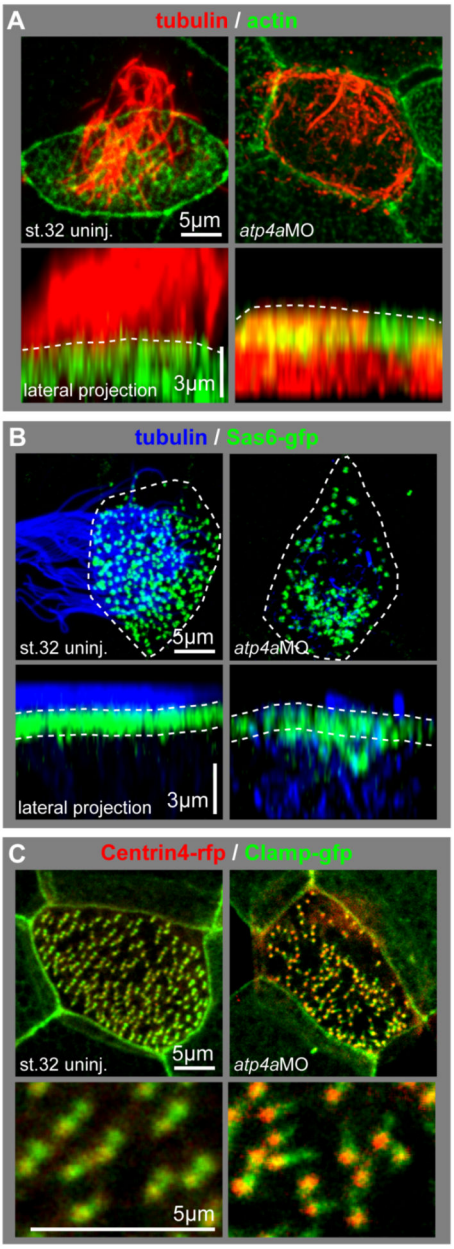

Fig. 2. Loss of ATP4 causes defects in MCCs reminiscent of foxj1 and Wnt/PCP phenotypes

(A–C) Analysis of the cellular phenotype in MCCs using high magnification confocal single cell imaging. (A) Cells were stained with an antibody against acetylated-α-tubulin (tubulin, red) and phalloidin-Alexa488 for actin staining (actin, green). Control (uninj.) MCCs were characterized by the presence of a dense ciliary tuft projecting from the apical surface (dashed lines in lateral projections) and the presence of an apical actin meshwork. In contrast, MCCs in atp4a morphants showed reduced ciliation, intracellular accumulation of tubulin and defects in the apical actin meshwork formation. (B) The localization of basal bodies to the apical membrane was analyzed using overexpression of sas6-gfp (green) in combination with tubulin (blue) staining, the outlines of the cells are depicted by the dashed lines in the apical views. Control MCCs were fully ciliated and basal bodies aligned close to

the apical membrane (dashed lines in lateral projections), while atp4a morphant MCCs had severe defects in ciliation, which correlated with aberrant basal body distribution within the cell. Basal bodies in atp4a morphants were mislocalized to the deep cytoplasm and not uniformly distributed along the apical membrane. (C) Basal body orientation was analyzed using centrin4-rfp (red) and clamp-gfp (green) overexpression. In control MCCs, basal bodies were mostly uniformly aligned along the anterior-posterior axis, while this alignment was randomized in atp4a morphant embryos. Lower panels show a magnified field of basal bodies.

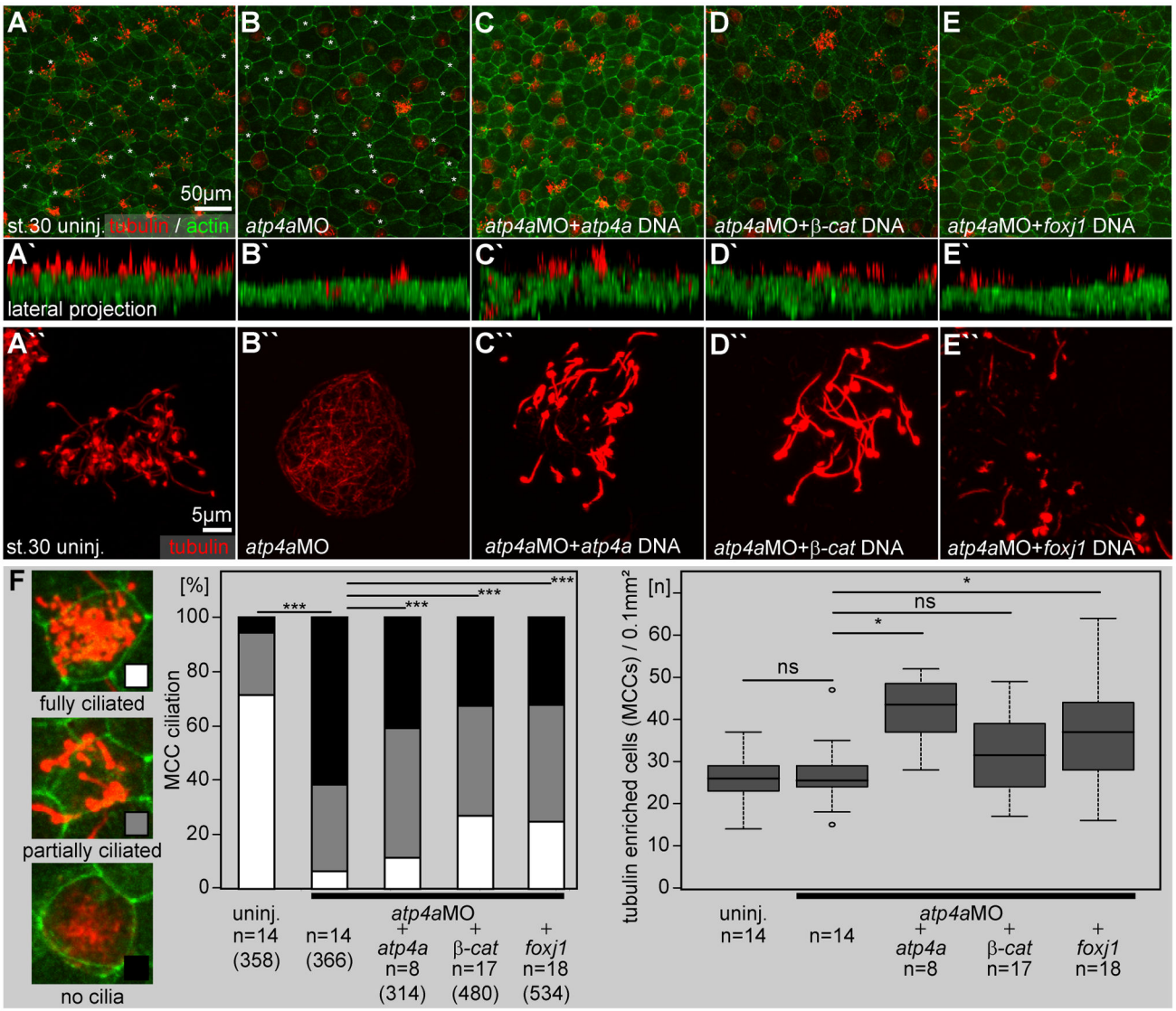

Fig. 3. ATP4-dependent Wnt signaling is required for foxj1 expression and ciliation in the Xenopus embryonic skin

(A–E) Immunofluorescent analysis of skin ciliation at stage 30. Embryos were stained for tubulin (acetylated-α-tubulin, red) and actin (phalloidin-Alexa488, green) and analyzed by confocal microscopy. (B) In atp4a morphants fully ciliated, partially ciliated and non-ciliated MCCs were found. Smaller intercalating cells with ISC morphology, which are also negative for acetylated-α-tubulin staining are marked with asterisks in A and B. Note that atp4a (C), β-catenin (β-cat.; D) and foxj1 (E) DNAs partially rescued ciliation in atp4a morphants. (A′–E′) Lateral projections of confocal Z-scans are shown in (A–E). (A″–E″) Higher magnification of representative MCCs. (F) Quantification of results.
n, number of embryos; (n), number of cells.

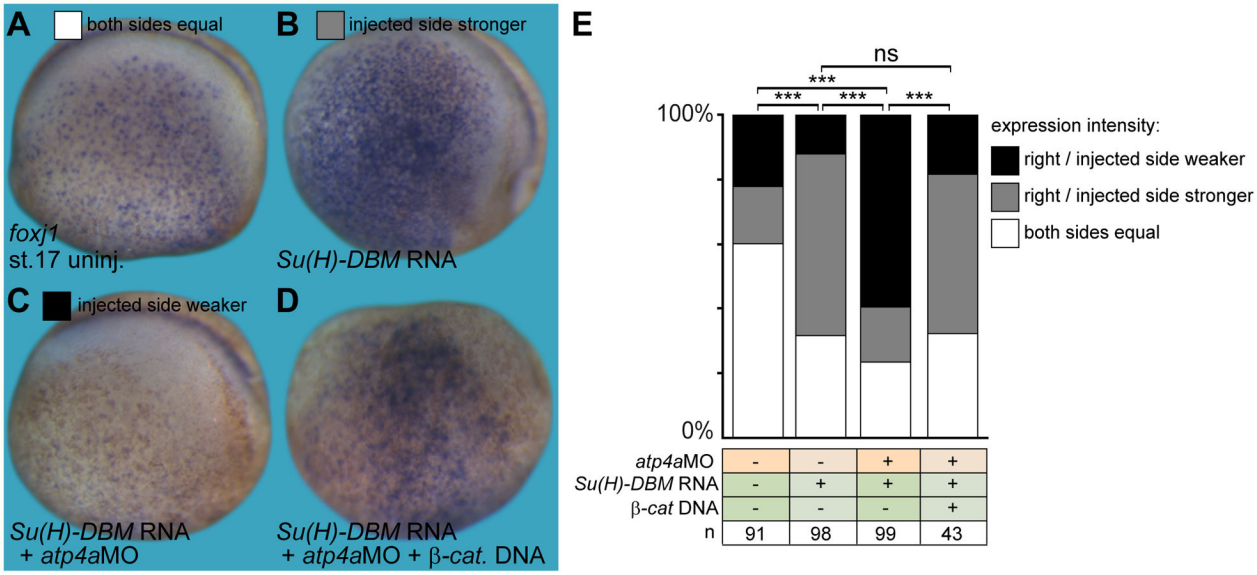

Fig. 4. ATP4a-dependent Wnt signaling acts downstream of Notch in skin foxj1 induction

(A–D) Foxj1 was stained in uninjected control (uninj.) embryos (A), as well as manipulated embryos (injected side shown in B–D). (B) Inhibition of Notch by injection of Su(H)-DBM mRNA increased foxj1 expression, which remained dependent on ATP4a (C) and Wnt/β-catenin (β-cat.; D). (E) Quantification of results. Staining intensity on the injected (right) side was compared to the uninjected (left) control side and quantified as right/injected side stronger, weaker or equal to the control side (G).

a, anterior; d, dorsal; n, number of embryos; ns, not significant; p, posterior; st., stage; v, ventral.

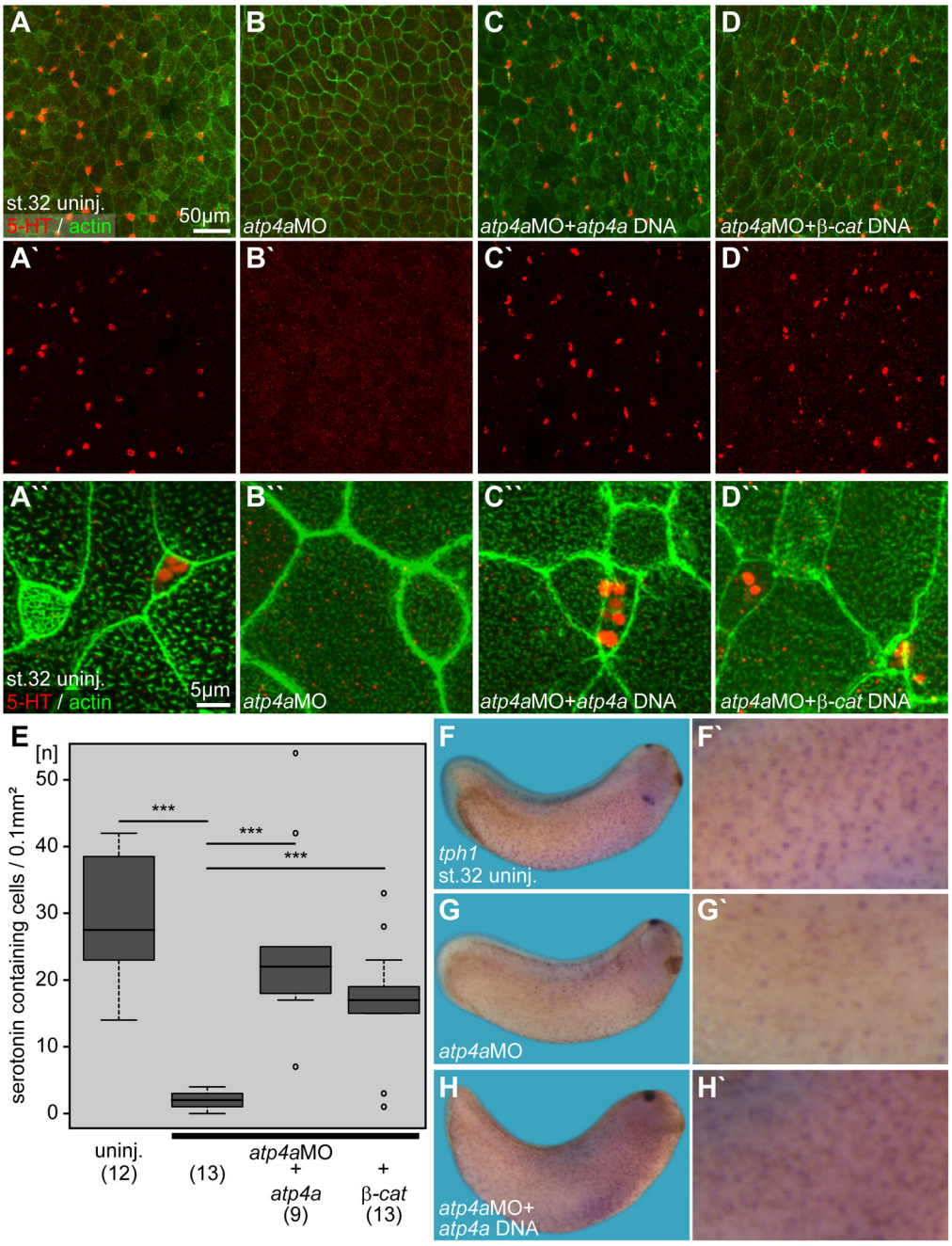

Fig. 5. Serotonin secretion and tph1 expression in the embryonic epidermis are regulated by ATP4a-mediated Wnt/β-catenin signaling

(A–D) Immunofluorescent analysis and quantification (E) of serotonin (5-HT; red) deposition in small secretory cells (SSCs) of the skin at stage 32. Actin (phalloidin-Alexa488) staining in green. (A) Uninjected (uninj.) control. (B) Loss of serotonin staining in atp4a morphants. (C, D) Rescue of serotonin staining upon co-injection of atp4a (C) or β-catenin (β-cat.; D) DNA constructs. (A′–D′) Serotonin channel. (A″–D″) Higher magnification of (A–D). (E) Quantification of results. (F–H) WMISH for tph1. (F, F′)

Uninjected control. (G, G′) Loss of tph1 expression in atp4a morphants was rescued by co-injection of atp4a DNA (H).
n, number of embryos; st., stage.

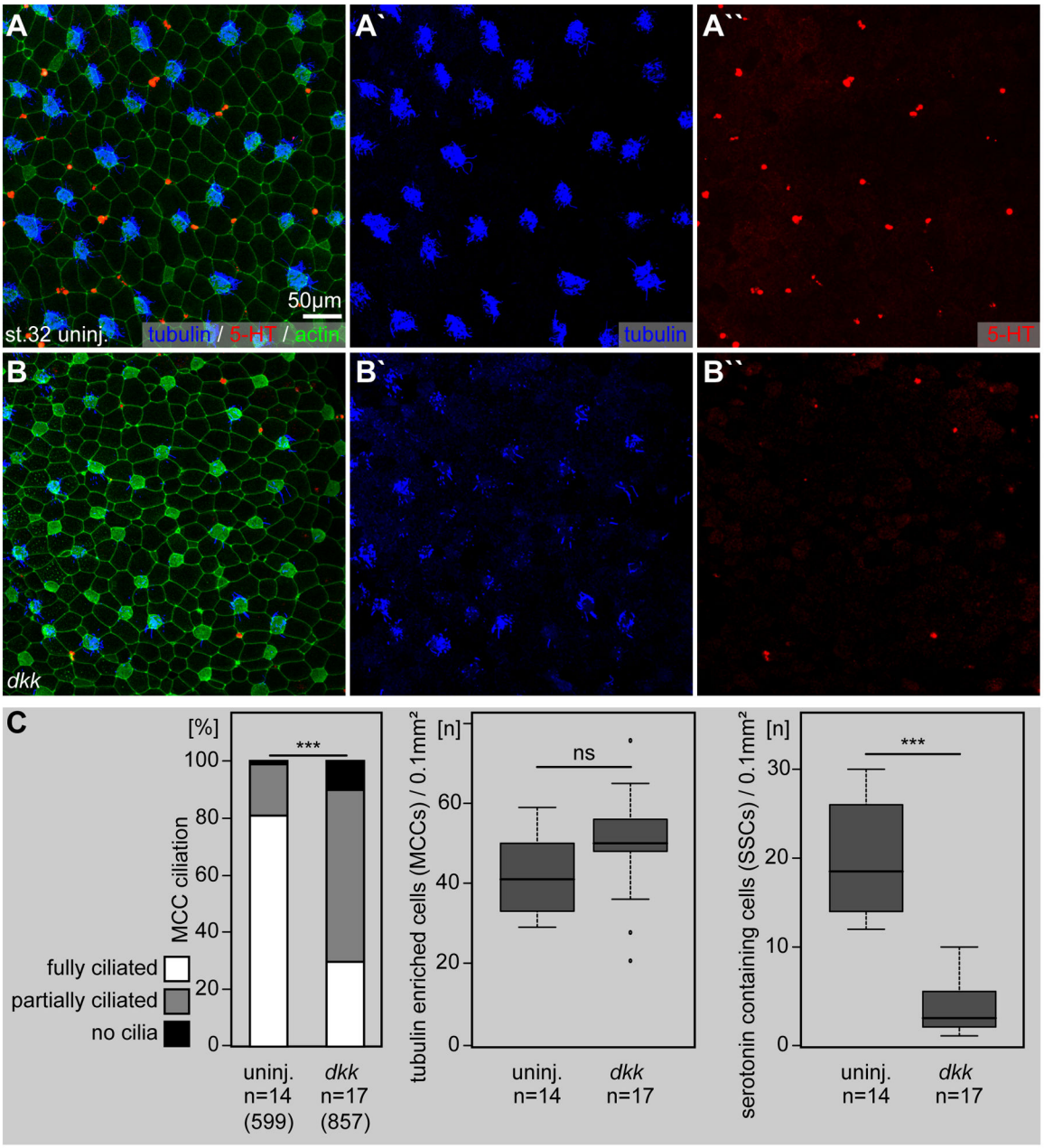

Fig. 6. Endogenous Wnt/β-catenin signaling is required for ciliation and serotonin signaling in the ciliated epidermis

Immunofluorescent analysis (A, B) and quantification (C) of MCC ciliogenesis (acetylated-α-tubulin, blue) and serotonin (5-HT; red) deposition in small secretory cells (SSCs) of the skin at stage 32. Actin (phalloidin-Alexa488) staining in green. (A) Uninjected (uninj.) controls are characterized by dense ciliation of MCCs (A′) and the presence of large numbers of serotonin positive SSCs (A″). (B) Impaired ciliogenesis and loss of serotonin staining in dkk injected specimens. dkk injected embryos showed a decrease in ciliation in MCCs (B′) and reduced numbers serotonin stained cells (B″).

n, number of embryos; (n), number of cells; st., stage.

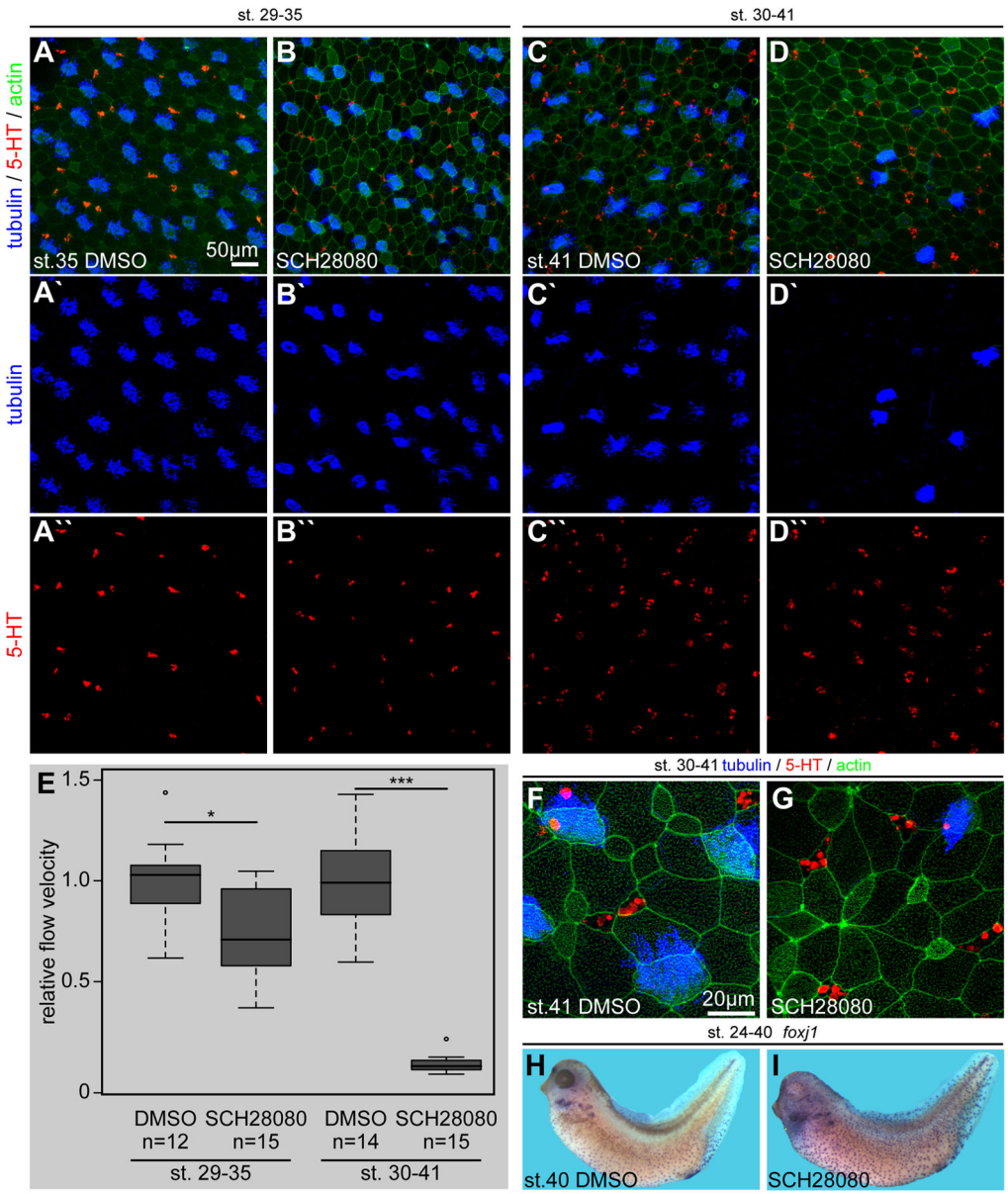

Fig. 7. Late pharmacological inhibition of ATP4 causes loss of MCCs and decreased mucociliary clearance

Immunofluorescent analysis (A–D) of MCC ciliogenesis (acetylated-α-tubulin, blue) and serotonin (5-HT; red) deposition in small secretory cells (SSCs) of the skin at stages 35 (AB) and 41 (C–D). Actin (phalloidin-Alexa488) staining in green. Embryos were treated with DMSO as control or SCH28080 during the indicated stages. Stage 35 (A) and stage 41 (C) DMSO treated controls displayed fully ciliated MCCs (A′, C′) and the presence of large numbers of serotonin positive SSCs (A″, C″). At stage 35 no apparent defects in MCC ciliation (B′) or SSC serotonin deposition (B″) were observed in SCH28080 treated embryos (cf. Quantification in Fig. S3K), although 50% of specimens contained MCCs with a relatively small apical surface area and 60% of specimens were abnormal in their epithelial morphology, i.e. enlarged cells were present (cf. Quantification in Fig. S3K). In contrast,

SCH28080 treatment until stage 41 lead to a massive loss of MCCs (D′), but no effect on SSCs (D″). (E) Quantification of cilia-driven fluid flow velocities revealed a significantly reduced extracellular fluid flow at the epidermis at stages 35 and 41, as compared to DMSO treated controls of the same stage. (F–G) High-magnification confocal imaging on the same set of specimens depicted in (C and D) confirmed the lack of MCCs, but intact SSCs in SCH28080 treated embryos and further indicated apical expansion in ISC-like cells and SSCs as well as enriched actin staining at some cell junctions (G). MCCs and epithelial morphology appeared normal in DMSO treated controls (F). (H–I) Embryos were treated with DMSO or SCH28080 from stage 24–40 and foxj1 expression was analyzed by in situ hybridization. In comparison to controls (H), foxj1 staining was increased in SCH28080 treated tadpoles (I).

n, number of embryos; st., stage.